An Elastomeric Poly(Thiophene-EDOT) Composite with a Dynamically Variable Permeability Towards Organic and Water Vapors

ARTICLE *in* ADVANCED FUNCTIONAL MATERIALS · AUGUST 2012

Impact Factor: 11.81 · DOI: 10.1002/adfm.201102237

8 AUTHORS, INCLUDING:

Brett D Martin
United States Naval Research Laboratory
30 PUBLICATIONS **789** CITATIONS
SEE PROFILE

Jawad Naciri
United States Naval Research Laboratory
129 PUBLICATIONS **2,508** CITATIONS
SEE PROFILE

Rhonda M. Stroud
United States Naval Research Laboratory
343 PUBLICATIONS **6,235** CITATIONS
SEE PROFILE

Banahalli Ratna
United States Naval Research Laboratory
193 PUBLICATIONS **4,586** CITATIONS
SEE PROFILE

FULL PAPER

An Elastomeric Poly(Thiophene-EDOT) Composite with a Dynamically Variable Permeability Towards Organic and Water Vapors

Brett D. Martin, Gusphyl A. Justin, Martin H. Moore, Jawad Naciri, Theresa Mazure, Brian J. Melde, Rhonda M. Stroud, and Banahalli Ratna**

An interpenetrating polymer network (IPN) material with controllable nanoporosity is developed for applications such as chemical protection. The IPN material is based on a conducting polymer backbone consisting of thiophene and 3,4 ethylenedioxythiophene (EDOT) repeat units–poly(thiophene-EDOT)–formed within a soft polyurethane support. The IPN demonstrates reversible, electrochemically switchable nanoporosity in the absence of standard liquid electrolyte, with the oxidized state being the open (high porosity) state and the reduced state being the closed (low porosity) state. The switching of the IPN between its oxidized (open) and reduced (closed) states is actuated using application of ±1.0 V. The variability in the IPN porosity, induced by the electrochemical switching, is revealed by large changes in water vapor diffusivity, as well as changes in the diffusivities of the chemical agent simulants chloroethyl ethyl sulfide (CEES) and methyl salicylate (MeS). The closed state of the IPN is able to decrease CEES diffusivity by ≈99% compared to expanded Teflon (ePTFE), while the open state allows high MVT rates comparable to ePTFE. The IPN's ability to allow high MVT under non-threat conditions (open state) and high protection from agents under threat conditions (closed state) is a unique and desirable characteristic of this novel IPN material.

1. Introduction

New materials with nanoscale porosities that can be reversibly changed between permeable and impermeable states on demand are of great interest in a variety of applications. They are expected to be useful in areas such as controlled release,[1–3] breathable protective clothing,[4] and intelligent sensing/filtration and separations processes.[5,6] Thus far, such materials under development exhibit permeability changes commonly triggered by stimuli such as electric fields,[6] redox,[7,8] pH,[9–11] light,[12] and temperature[3] and are generally performed under aqueous conditions. The physical mechanism underlying such changes in permeability is often based on the reversible swelling and shrinking of solvated polymer networks, the coiling and uncoiling of polymer chains (polymer brushes) or the association and disassociation of polymer chains attached to porous surfaces.[5]

Fu and colleagues reported control over the pore sizes of mesoporous silica particles modified with a stimuli-responsive polymer, poly(N-isopropyl acrylamide) (PINPAAm).[3] The thermoresponsive polymer was used to demonstrate controlled release of rhodamine dye from the silica particles. Stimuli-responsive polymers that use pH for control over the gating mechanism have also been investigated, where gating relies on charge repulsion between polyionic tethers.[10,11] In these experiments the authors covalently attached amine-containing tethers to the surface of a mesoporous substrate, silica MCM-41. Protonation of the amines resulted in like-charge repulsion, causing the polyionic tethers to extend over the mesopore openings, blocking them and inhibiting the transport of dye across the mesoporous silica. Amine deprotonation reversed the process, opening the mesopores. Similar types of reversible gating mechanisms that use grafted polymer brushes of mixed types have been explored as well.[13] Approaches such as these have the limitation of relying on a specific solution property (such as pH, ionic strength and temperature) for the gating action to occur.

The bulk transport characteristics of conducting polymers can often be changed by applying a small voltage, which alters the redox state of the polymer.[4,14–16] In some cases, this can cause large variations in the diffusion coefficients of solutes[4] or colloidal particles.[16] For example, selective transport and gating of nanopores using vertically aligned carbon nanofiber

Dr. B. D. Martin, M. H. Moore, Dr. J. Naciri,
Dr. B. J. Melde, Dr. B. Ratna
U. S. Naval Research Laboratory
Center for BioMolecular Science and Engineering
Code 6930, Washington, DC 20375, USA
E-mail: brett.martin@nrl.navy.mil; ratna@nrl.navy.mil
Dr. G. A. Justin
Crosslink, TM, 950 Bolger Ct
St. Louis, MO 63026, USA
T. Mazure
Nova Research Inc.
1900 Elkin St. #230, Alexandria, VA 22308, USA
Dr. R. M. Stroud
U. S. Naval Research Laboratory
Code 6366, Washington, DC 20375, USA

DOI: 10.1002/adfm.201102237

(VACNF) membranes coated with electropolymerized polypyrrole (PPy) has been demonstrated.[16] Electrochemical reduction of the conducting polymer led to swelling of the VACNF nanofibers, resulting in a decrease in the membrane pore size. The large dopant anion, dodecylbenzyene sulfonate (DBS), was entrapped within the polymer matrix during polymerization, and acted to balance the positive charge of the oxidized polymer. When the conducting polymer was reduced, cations rapidly diffused in to balance the excess negative charge (DBS) in the polymer, resulting in swelling. The pore size in the membrane was shown to decrease from 250 to 350 nm to ~50 to 250 nm after swelling. Various applications of such a nanoporous membrane were cited by the authors to include separations, molecular sensing and drug delivery. A major challenge identified in this work was the construction and integration of the nanoporous membranes within multiscale systems, while simultaneously and precisely controlling the selectivity of the membrane and the transport of small particles.

A number of studies demonstrating controlled release of small molecules from conducting polymer matrices have been reported, including the development of electrically actuatable nanoporous membranes for drug release.[17,18] Jeon and colleagues fabricated an actuatable porous membrane by electrochemical polymerization of polypyrrole (PPy) doped with DBS anion on a porous anodized aluminium oxide membrane.[17] The pore size was actuated by the large volume changes experienced by PPy/DBS during electrochemical switching. Using atomic force microscopy (AFM), the average pore diameters of the oxidized and reduced states were found to be 190 and 140 nm, respectively. This redox-controlled swelling and contraction behavior of polypyrrole has previously been described by Smela and colleagues.[19] As much as a 35% increase in the volume of DBS-doped PPy was observed and was attributed to the movement of solvated ions into the polymer upon reduction. In another study, Abidian and colleagues used electropolymerized poly(3,4 ethylenedioxythiophene) (PEDOT) nanotubes to demonstrate controlled release of dexamethasone.[18]

Apart from the volume changes described by Smela, Jeon and others, evidence suggests that surface effects may also play a role in the electrochemical actuation of diffusion processes in conducting polymers. Halldorsson and colleagues described the controlled transport of dichloromethane through DBS-doped polypyrrole (PPy-DBS) polymerized on a platinum mesh.[14] The ability of dichloromethane droplets to pass through the conducting polymer membrane upon electrochemical switching (reduction) was thought to arise from the release of the surfactant dopant into the dichloromethane and the change in the surface energy/wettability of the conducting polymer material. In the oxidized polymer state, the dichloromethane droplets had contact angles of about 120°. In the reduced state, the contact angle was 150°. A number of other chlorinated solvents, including trichloroethane, chloroform, and dichloromethane demonstrated similar contact angle changes upon electrochemical switching of PPy-DBS (oxidizing and reducing potentials of +0.6 V and −0.8 V vs. Ag/AgCl, respectively). The release of the surfactant from the reduced polymer decreased the surface tension of the solvent droplet, reducing the capillary effects that prevent the drop from penetrating the porous membrane. Due to the fact that solvent penetration occurred almost immediately upon reduction, well before surfactant could be released from the surface of the conducting polymer, it was suggested that changes in the PPy surface energy were also a contributing factor to the dichloromethane transport.

Thus far, the vast majority of nanoporous membranes with electrically switchable permeability are able to influence transport in the liquid phase only. The significance of our work described here is that we have developed a conducting polymer composite material that demonstrates desirable mechanical properties such as high strength and flexibility, while also demonstrating electrically switchable permeability, in a macroscopically "dry" state, to species in the gaseous phase. To the best of our knowledge, it represents the first switchable material able to reversibly control the diffusion of a vapor-phase species.

An important goal of this work was to support the development of a dynamic material that could be used in protective clothing. The fabric should be capable of "switching" from an open "breathable" state that is comfortable to wear to a closed, protective state that can block transport of toxic vapors such as chemical warfare agents. The development of the material began with the synthesis of a tether-containing thiophene monomer with a charged terminus, and its electrochemical polymerization on gold surfaces.[4] In this earlier work, we synthesized and characterized the tether-containing polythiophene conducting polymer poly(3-{2-[2-(2-{2-[(thiophene-3-carbonyl)-amino]-ethoxy}-ethoxy)-ethoxy]-ethoxy}-ethane-1-sulfonic acid), or poly(TP-CAE_5-SO_3). Electrochemical studies showed that this conducting polymer strongly influenced the diffusivities of electrolyte ions as its redox states were electrochemically switched. The mechanism of influence on ion diffusivity was thought to result from mechanical obstruction and clearance by the sulfonate-terminated tethers and mediated by "self-doped" (oxidized state) and "de-doped" (reduced state) configurations. Control experiments using a simple methyl-substituted polythiophene without tethers showed no similar effects on ion diffusion.

We report here a novel conducting polymer composite material that is based on the tether-containing thiophene described above. The composite is able to control the diffusivities of vapor-phase species through an electrical switching process performed in the macroscopically dry state - that is, in the absence of conventional liquid electrolyte. The composite is an interpenetrating network (IPN) material composed of soft polyurethane interspersed with a crosslinked poly(thiophene-EDOT)-based conducting polymer. The tether functionality is attached to the thiophene repeat units. The IPN is formed in a mechanically strong fabric support.

2. Composite Formulation

The composite material was designed to be reversibly "switchable" between its oxidized and reduced states by the application of a small voltage. When the network is "switched", in our paradigm the moveable tethers respond by forming ion-pairing complexes that either increase or decrease the material's meso- and nanoscale porosity. The material thus has an "open" state that has a high porosity, and a "closed" state with a lowered porosity. Most importantly, 1) the material can be "switched" between its redox states in the absence of a bulk liquid electrolyte, and

2) both the "open" and "closed" states are maintained indefinitely without the continued application of voltage.

The composite architecture comprises a number of components that, in our view, are essential for manifestation of the open-close (nanogating) behavior, and the mechanical strength/coherence of the material: 1) electrically conducting poly(thiophene-EDOT) main chains; 2) oligoethylene glycol (OEG) side chains each bearing a sulfonate terminus (tethered counterion); 3) EDOT-ODA-EDOT crosslinker (ODA refers to the octanedioate bridge between the two EDOT moieties); 4) polyurethane scaffold; 5) room temperature ionic liquid (RTIL); 6) conducting carbon fibers, and 7) the support fabric. The IPN precursors are shown in **Figure 1**a–d, and the final IPN constituents are depicted in the boxed Figure 1e–g. The crosslinked conducting polymer (CP) portion (Figure 1e) is formed as a statistical terpolymer, in the presence of the polyurethane support (Figure 1f). The relative amounts (wt%) of each component in the final, fabric-supported composite are shown in Figure 1h. The weight ratio of IPN to support fabric is ~40:60. A suggested redox switching mechanism is depicted in Figure 1i, where the tethered sulfonate participates in an intramolecular "self-doping" charge balance as the polymer enters its oxidized form. Similar redox behavior of CPs such as polythiophenes and PEDOT has been described in previous literature.[19]

We chose polythiophene derivatives for the conducting polymer because they have been shown to be environmentally stable over long time periods (i.e. months) in various applications such as field-effect transistors, in the presence of oxygen and water vapor.[20] The derivative 3,4 ethylenedioxythiophene has been shown to be suitable in copolymerization schemes with thiophene and closely-related compounds.[21,22]

The selection of the OEG moiety (see Figure 1a) to serve as the tether was made because of several unusual attributes. These include its high flexibility as a molecular chain, which gives it a large configurational entropy that allows it to adopt many chain configurations. In the tether-containing monomer 3-{2-[2-(2-{2-[(thiophene-3-carbonyl)-amino]-ethoxy}-ethoxy)-ethoxy]-ethoxy}-propane-1-sulfonic acid ("TP-CAE_4P-SO_3", Figure 1a), a propyl group links the sulfonate moiety to the OEG portion. Polymers such as poly(TP-CAE_5-SO_3) and poly(TP-CAE_4P-SO_3) are expected to have characteristically large chain entropies.[23] This should enhance the self-doping ability of the anionic terminus and the ability of the chain to block diffusing guest molecules. Also, there is a growing body of literature describing the behavior of comb polymers based on poly(OEG-methacrylate).[24] They often show unusual aggregation/dissociation behaviors that arise from the interplay between hydrophilic (OEG-mediated) and hydrophobic (methacrylate-mediated) forces. Related processes may assist in mechanisms underlying the dynamically variable nanoporosity in the IPN described here. Also, it has been convincingly demonstrated that glycols and related compounds can enhance the conductivities of oxidized PEDOT.[25,26] Finally, it is known that asymmetrically substituted OEG chains can facilitate cation transport,[27] another effect that may contribute to the conductivity of the IPN polymer. A sulfonate was selected as the OEG terminus since it is a classical dopant anion choice for many types of CPs, [28] and has been used in self-doping schemes for polythiophenes and PEDOTs.[29]

The purpose of the EDOT-ODA-EDOT crosslinker (Figure 1b) was to contribute to the mechanical strength of the polymer and prevent liquid-phase dissolution of the poly(TP-CAE_4P-SO_3) chains. The crosslinker was designed with two considerations in mind. First, the alkane crosslinking chain was made short enough so that the two EDOT moieties would not be able to easily couple with one another during polymerization. Second,

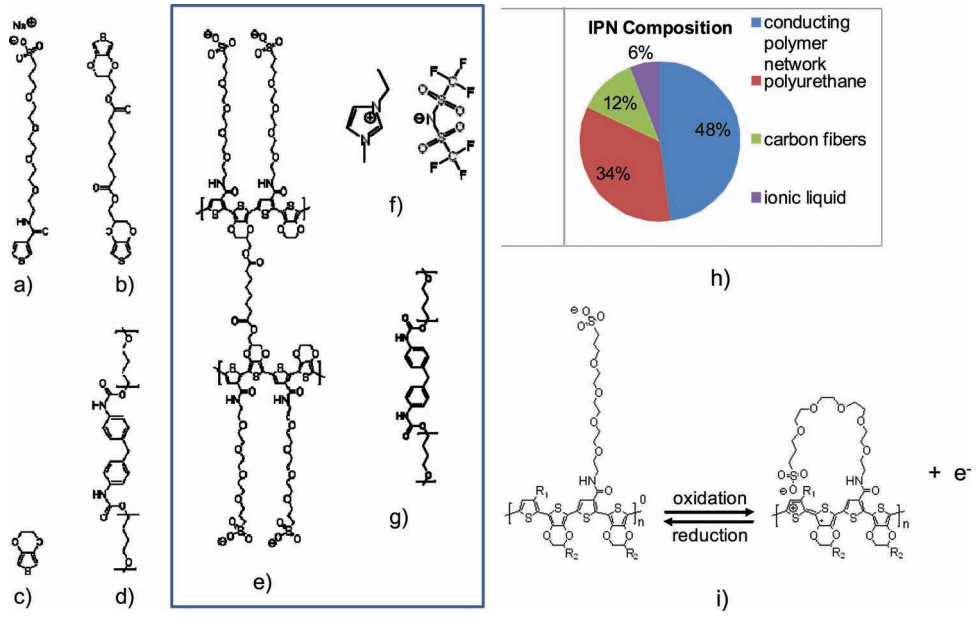

Figure 1. a–g) IPN components. IPN precursors (a–d); components of the final IPN (e–g). e) Poly(thiophene-EDOT) with TP-CAE_4P-SO_3 tether-thiophene, f) room-temperature ionic liquid Emim-Tf_2, g) polyurethane support. h–i) IPN composition by weight (h) and proposed redox switching of the conducting polymer backbone (i). "R_1" denotes tether side-chain and "R_2" denotes alkyl chain crosslinker or hydrogen atom, omitted for clarity.

it was made to have roughly the same length as both the TP-CAE_4P-SO_3 tether-thiophene as well as the "hard" crosslinking segment of the polyurethane component (the methylene-bridged bis-benzamide, Figures 1d,g). It was thought that the similarities in length would lead to a greater degree of homogeneity in the final IPN molecular structure. The density of the crosslinker was chosen so that the number of EDOT repeat units equaled the number of thiophene repeat units in the finished IPN (Figure 1e), an attribute that was also thought to enhance the homogeneity of the final IPN molecular structure. To obtain this ratio, underivatized EDOT was also included (Figure 1c).

The polyurethane support (Figure 1d,g) was chosen for its innate ability to transport water vapor, and its observed compatibility with the tether-containing conducting polymer. Water vapor transport rates are an important consideration in the design of breathable protective clothing. The polyurethane component contributes to the elasticity and mechanical strength of the IPN. Its chemical composition and "free volume" (interconnected nanoporosity) allow it to have relatively high moisture vapor transport capabilities.[30] It is a thermoplastic polymer based on aromatic and ether repeat units, and is compatible with the CP polymerization and redox chemistries. During the oxidative polymerization of the CP, it slowly precipitates as the polymerization solvent evaporates, encasing the polymerized CP and forming the IPN.

Our end goal was to develop an IPN that could be switched between high- and low-permeability states while in a macroscopically "dry" (solvent-free) condition. In the absence of liquid phase electrolyte, electrochemical switching of conducting polymers is very difficult. To facilitate the switching process, a small volume (~6 wt% of the IPN) of room temperature ionic liquid was introduced into the material after synthesis (Figure 1f). This corresponds to about a 1:1 molar ratio with the OEG-sulfonate tether. The ionic liquid, 1-ethyl-3-methyl imidazolium-bis-(perfluoroethylsulfonyl) imide (Emim-Tf_2), was introduced as a 30 wt% solution in ethanol. Emim-Tf_2 has an extremely low vapor pressure, and essentially only the ethanol evaporates from the IPN, leaving the Emim-Tf_2 behind as a long-term component of the IPN. Ionic liquids have previously been incorporated into conducting polymers such as PEDOT[31,32] and have been shown to improve their properties, including switchable conductivity and wettability. They have also been shown to improve the conductivity of elastomeric conducting polymers.[33]

Micrometer-scale conducting carbon fibers (~50/5 μm length/diameter) were added to the IPN polymerization solution, and comprise ~10% of the weight of the finished IPN. They are included to improve charge percolation, and are also thought to increase the electric field strength and distribution in the IPN when the switching voltages are applied. Their presence in the polymerization solution causes its viscosity to increase slightly, which we have found improves its processability.

Non-woven nylon (pore size of 0.1 μm) was chosen as a support fabric for the IPN. The nylon is mechanically strong and does not appear to be degraded by the polymerization solvent or the iron (III) oxidant. It is also not thought to be involved in the IPN switching (open-close) process. We are currently investigating other support fabrics as well, including wool and polyester, which are both suitable as support fabrics.

3. Results and Discussion

3.1. Electrical Impedance Spectroscopy

Electrochemical impedance spectroscopy (EIS) was performed on the composite material in both its putative open (oxidized) and closed (reduced) states to verify electrochemical switching of the IPN. The material generated profoundly different EIS responses between the two redox states of the conducting polymer. EIS was conducted within a frequency range of 10^5 to 10^{-2} Hz with an applied peak to peak potential (V_{pp}) of 10 mV. The material was switched to its reduced state by application of a −1.0 V potential to the working electrode, for an appropriate period of time until a charge of ~0.1 C had been passed. The switching was performed in this way since it is desirable in the final application (protective clothing) to create a system where the material can be switched between open and closed states using a simple electrode configuration. We performed initial EIS measurements on the synthesized, fully polymerized oxidized IPN, followed by measurements on the material in its reduced state. The results showed impedances that were about one order of magnitude lower in the oxidized vs. the reduced states. Impedance values of 500 Ω −1kΩ were recorded for the former state, while higher values (~7 kΩ) were recorded for the latter. The Bode impedance plots (|Z| vs. frequency) for each of the two states demonstrate very nearly frequency-independent behavior across the entire frequency range interrogated (**Figure 2**a). The Nyquist plot for the oxidized state

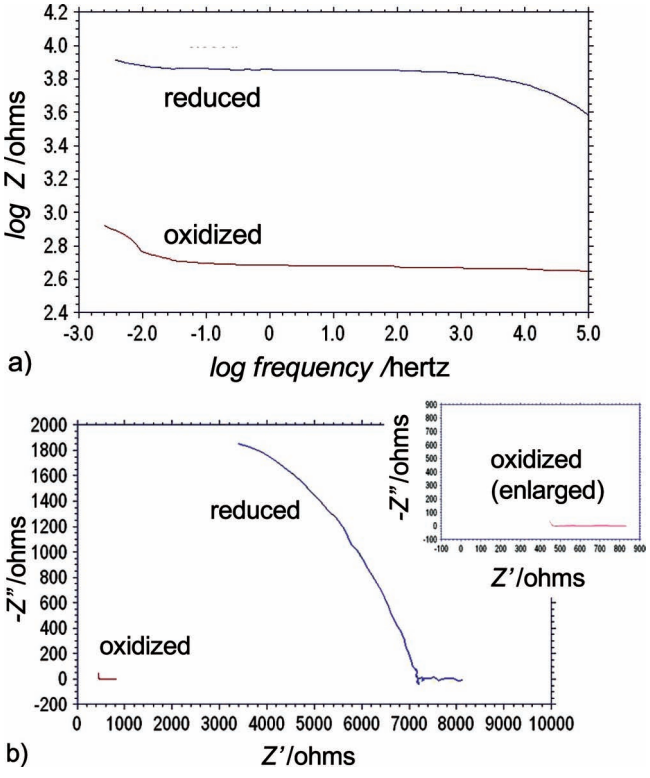

Figure 2. a) Bode impedance plots of the IPN in its reduced (putative closed, high impedance) and oxidized (putative open, low impedance) states. b) Nyquist plots of the IPN in its oxidized and reduced states.

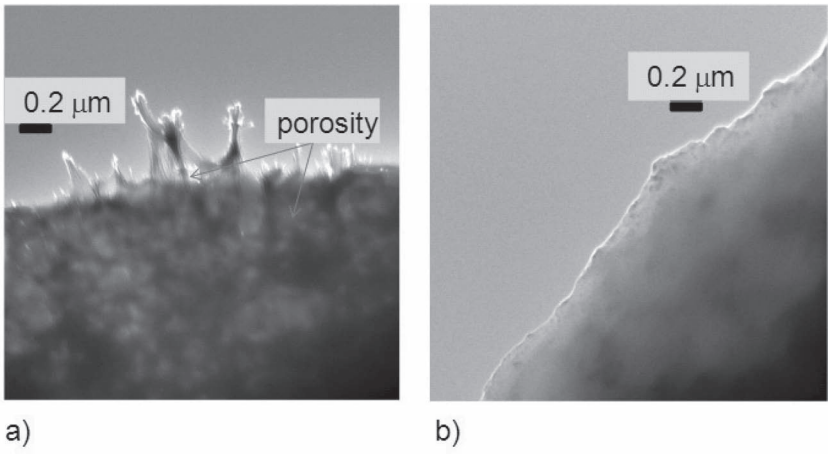

Figure 3. TEM images of the IPN in its a) oxidized (open) and b) reduced (closed) states.

demonstrates almost pure resistive behavior (Z″ ~ 0) across all frequencies. However, the plot reveals that a significant increase in both the real (resistive) and imaginary (reactive) components of the impedance occurs when the material is switched from its oxidized to its reduced form. An equivalent circuit of the IPN material connected on opposite sides by the working and counter electrodes can be approximated as a resistor in parallel with a capacitor, with Z′ and Z″ described by the following equations:

$$Z' = \frac{R_p}{1 + \omega^2 R_p^2 C_p^2} \quad (1)$$

$$Z = \frac{-\omega R_p^2 C_p}{1 + \omega^2 R_p^2 C_p^2} \quad (2)$$

where Z' and Z'' are the real (resistive) and imaginary (reactive) components of impedance, ω is the angular frequency, and R_p and C_p are the resistance and capacitance of the material, respectively. Using current measurements with Ohm's Law, values of R_p were determined. For the oxidized state of the material, R_p was found to be 570 ± 90 Ω, whereas for the reduced state R_p was found to be 1714 ± 255 Ω. From Equation 1, 2, at a frequency of 1 Hz, C_p was found to be 14.4 ± 2.3 mF/gram composite for the oxidized state and 0.165 ± 0.025 mF/gram composite for the reduced form. Since conducting polymers such as PEDOT and poly(thiophene) are more conducting in their oxidized vs. reduced states, it was reasonable to assume that the same would be observed for our material. As expected, when the IPN polymer was switched from its oxidized to its reduced state, R_p increased. As a consequence, Z' became more positive (via Equation 1). Also, Z'' became more negative (via Equation 2), as is observed in Figure 2b. The higher C_p of the oxidized state may arise from the polyionic nature of the conducting polymer backbone, combined with an inherently higher nanoporosity, which could allow easier charge movement. The EIS results support the hypothesis that the oxidized state has an "open" nature (higher nanoporosity), while the reduced state has a "closed" one (lower nanoporosity).

3.2. Transmission Electron Microscopy (TEM)

Transmission electron microscopy (TEM) was used as a direct means of visualizing the oxidized and reduced states of the IPN material, in expectation of discernable "open" and "closed" states. Suitable material samples were prepared by casting the IPN onto copper TEM grids or copper wire, and introducing the proportionate amount of the Emim-Tf_2 room temperature ionic liquid (RTIL). Samples were switched to their reduced state by carefully attaching the working, counter, and reference electrodes in the manner described above and subjecting them to a reducing voltage of −1.0 volts. EIS was routinely employed to verify whether this state had actually been attained. The TEM image of the oxidized as-synthesized state is shown in **Figure 3**a, and that of the reduced state is shown in Figure 3b. The oxidized state clearly has what appears to be regions of high and low porosity–large areas of light and dark regions, which represent electron-deficient and electron-rich regions, respectively. Together, they form an image resembling a sponge-like porous structure. The oxidized state poresize distribution may be in the meso- and nanoscale range. The reduced state (Figure 3b) is morphologically very distinct from the oxidized state. It does not show the sponge-like characteristics of the latter, but instead resembles a dense homogeneous phase with no evidence of porosity. The images of the two states are consistent with the model introduced above, and further discussed below. Because of this visual evidence and the EIS results, from this point onwards we will refer to the oxidized state as "open" and the reduced state as "closed".

3.3. Nitrogen Absorption Studies

To further characterize the open and closed states of the IPN, mesopore area measurements were undertaken using BET nitrogen adsorption techniques. The results are given in **Table 1**, which shows that the average pore surface areas are ~3.5 to 4.5-fold higher in the open vs. closed states of the material. This is an indication that the former state has larger average mesopore sizes than the latter, and likely provides diffusion pathways that are accessible and will allow rapid transport of small compounds.

Table 1. Mesopore surface areas for the oxidized (open) and reduced (closed) states of the IPN, as measured by nitrogen adsorption.

	IPN pore surface areas	
	Oxidized, open[a)] state	Reduced, closed state
Single point surface area at $p/p^\circ = 0.220$	3.44 [m^2/g]	0.970 [m^2/g]
BET Surface Area:	3.82 [m^2/g]	0.961 [m^2/g]
Langmuir Surface Area:	5.63 [m^2/g]	1.21 [m^2/g]

[a)]as-synthesized

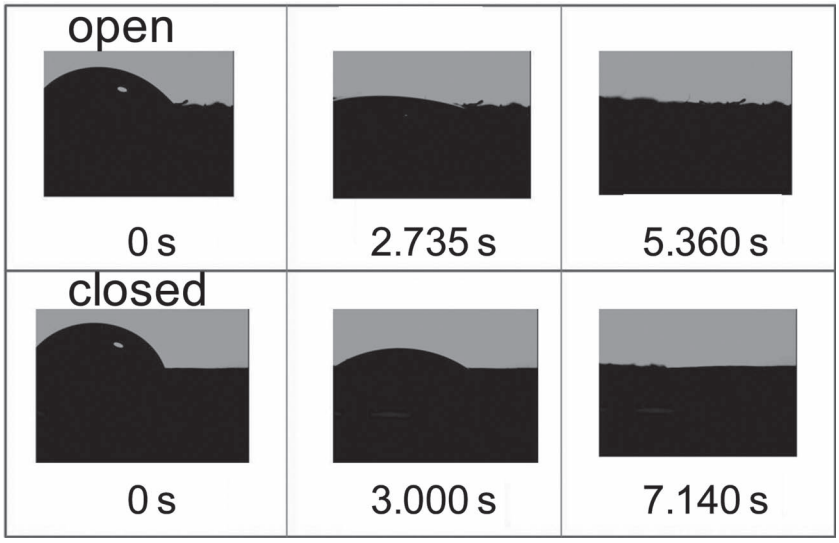

Figure 4. Time lapse photography of water droplets absorbed by fabric-supported IPN samples in their oxidized, open (top) and reduced, closed (bottom) states. In its open state, the IPN absorbed the water droplet at a rate of 1.5 (±0.3) μL s^{-1}, while in its closed state, the rate of absorption was 1.1 (±0.3) μL s^{-1}.

3.4. Liquid Water Absorption Rates

Next, we wished to quantify surface hydrophilicity effects that may be associated with the two IPN states. Conducting polymers are sometimes known to undergo reversible changes in wettability as they are switched between redox states. This has been attributed to effects of the counteranions as they ion-pair with the CP main chain during charge-compensation. The wettability of conducting polymers has been shown to be largely affected by the type of dopant anion used.[34] For example, polypyrrole (PPy) films with large perfluorinated dopant anions were shown to demonstrate high hydrophobicity (water contact angle > 90°) while perchlorate (ClO_4^-) doped PPy was shown to be hydrophilic.[35] However, it is also known that poly(3-methylthiophene) can be switched between a hydrophilic conducting (oxidized) state and hydrophobic neutral (reduced) one using perchlorate as the dopant anion, and the two states were used to either absorb or repel charged micelles in aqueous solution.[36] Thus, both the nature of the dopant anion and the intrinsic hydrophilicity of the conducting polymer itself can strongly influence the bulk hydrophilicity of the surface.

To obtain information regarding the hydrophilicity/hydrophobicity of the open (oxidized) and (closed) reduced states of the material, we used time lapse video to record the absorption of water by the IPN material, supported by fabric. Since a known volume of liquid was applied to the surface, the rate of absorption could be calculated (volume/time). A hydrophilic material will be expected to absorb the water droplet faster than a more hydrophobic one. It was found that the material absorbed the water droplet much more rapidly in its open than in its closed state (**Figure 4**). In the open state, the rate of absorption was about 1.5 (± 0.3) µL s^{-1}, while for the closed state, the absorption rate was 1.1 (± 0.3) µL s^{-1}. Although there is some uncertainty arising from the experimental error, these results do support the expectation that the conducting polymer is more hydrophilic in its oxidized open state, favoring better wettability of the IPN and consequently more rapid water absorption, than in the reduced closed state. This may also be a direct consequence of the larger pore areas in the open vs. closed state, and furthermore may be related to CP chain rearrangements (packing) that occur during redox switching. These are known to occur in PEDOT-type CPs,[37] a point which will be discussed later. Finally, gradual migration of lower-MW material components may affect the water absorption rates through the surface, a possibility that we are continuing to investigate.

3.5. Synthesis of Control IPN

To allow comparison of the tether-containing IPN ("Tether-IPN") to a similar material without tethers, we synthesized a "Control-IPN" wherein the TP-CAE_4P-SO_3 and EDOT repeat units were replaced with 3′ 4′-dimethyl-[2, 2′; 5′, 2″]-terthiophene (DMTP) and crosslinked with EDOT-ODA-EDOT. The Control-IPN was synthesized in a manner similar to that for the tether-containing IPN, and was formed in a nylon support. The Emim-Tf_2 RTIL was added in a manner identical to that for the Tether-IPN. We were thus able to attempt a dry-state redox switching of the material, as was done with the Tether-IPN. The distribution of IPN components corresponded to that for the Tether-IPN, which is depicted in Figure 1h. The structure of the DMPT-based conducting polymer and the Control-IPN polymer composition is illustrated in **Figure 5**

3.6. Moisture Vapor Transport Rates

As mentioned previously, for the material to be useful in eventual applications involving protective clothing, it must be comfortable to wear in its open state. One of the key determinants of fabric comfort is "breathability", which is strongly associated with a high water (moisture) vapor transport rate. We began characterization of the nylon-supported Tether-IPN in terms of its moisture vapor transport (MVT) ability, as well as its ability to inhibit organic vapor diffusion. For both characterizations, diffusion is reported as a dimensionless parameter (ratio versus a suitable control) rather than actual mass fluxes (mass per unit area per unit time).

MVT measurements were performed across each nylon-supported IPN sample (Tether-IPN oxidized, Tether-IPN reduced, Control-IPN oxidized, Control-IPN reduced) secured in a two-chambered diffusion cell (see Supporting Information Figure S1). Using flow controllers, the relative humidity (RH) in the right-hand chamber was adjusted to 25%, 50%, and 80% at 40 °C while the RH in the left-hand second chamber was recorded. This allowed us to determine the amount of water vapor passing through the sample as a function of time.

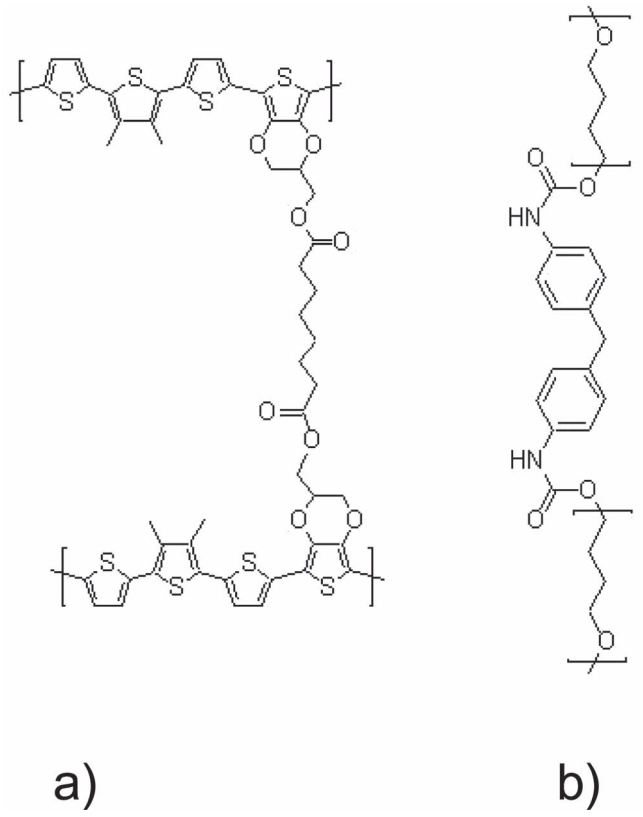

Figure 5. Control IPN polymer components. a) DMTP crosslinked with EDOT-ODA-EDOT and b) polyurethane support.

The ratio of MVT for each IPN sample vs. expanded Teflon (ePTFE) (MVT of IPN/MVT of ePTFE) is shown as a function of RH (25, 50 and 80%) in **Figure 6**. ePTFE transports water vapor at very high rates compared to other clothing materials.[38] The open IPN allows MVT at nearly the same rate as that of the ePTFE. For this set of experiments, the standard deviation ranged from ± 9% to 13%. The closed IPN allows significantly

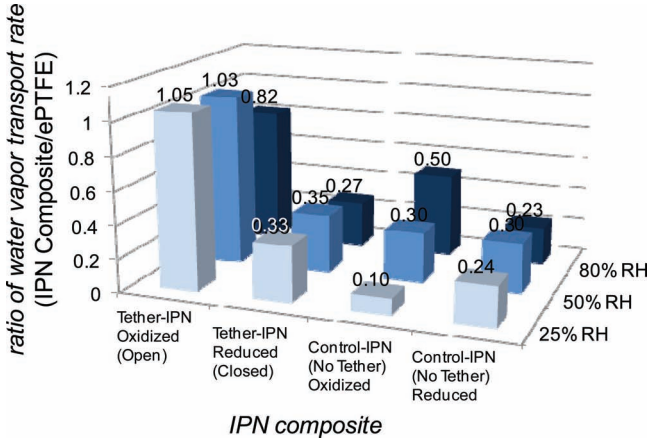

Figure 6. Comparison of moisture vapor transport (MVT) rates. The IPNs in their oxidized and reduced states are compared, versus expanded Teflon. T = 40 °C. Error bars are ±9-13%.

(~70%) less MVT, indicating that it can hinder transport of molecules as small as water. This result is consistent with the TEM images that indicate large differences in pore sizes between the open and closed states. It is also interesting that for both the open and closed states, MVT rates are nearly independent of RH. This is in contrast to the MVT characteristics observed for other types of breathable fabrics.[39] MVT through the Control IPN in its oxidized state was significantly lower than the Tether IPN, and appeared to have some dependence on relative humidity. MVT through the Control IPN in its reduced state was comparable to the Tether-IPN in its reduced state and did not demonstrate RH dependence. These results suggest that the presence of the tether facilitates the desirable characteristic of high MVT in the Tether-IPN open state. However, MVT is significantly diminished in its closed state. The high MVT of the oxidized state of the Tether-IPN compared to the Control IPN, and the comparable MVT in both reduced states suggests that the tether plays an important role in creating a pore structure that is conducive to high MVT through the Tether-IPN open state. The MVT through the closed state of the Tether-IPN is nearly identical to that through the reduced Control-IPN. Therefore, in the closed state of the Tether-IPN, the tether itself appears to play a minimal role in MVT.

3.7. Simulant Diffusion

We tested the Control-IPN and Tether-IPN materials using vaporized chloroethyl ethyl sulfide (CEES), which is a standard simulant for CW mustard agent. We used a continuous flow apparatus with flame ionization detection (Supporting Information Figure S1). This enclosed, temperature-controlled computerized test apparatus allowed us to perform diffusivity studies on the IPN composite membrane materials that involve the simultaneous presence of simulant vapor and water vapor. To begin the diffusion tests, the IPN was placed and sealed into the vapor diffusion chamber, made of glass. A small volume of liquid CEES was then injected through a septum into the left-hand chamber, which was held in a quiescent state (no convective airflow was present). During the course of the experiment, the CEES droplet rested on the end of the injection needle until it completely evaporated. A convective airflow with 50% relative humidity was passed through the right-hand chamber at a rate of 75 cm^3/min. The CEES vaporized and a portion of it passed through the IPN. The flowing air quickly carried this portion away from the membrane, preventing any backward diffusion. The airflow entered a flame-ionization detector (FID), and the amount of CEES present was detected as a time-dependent peak. The portion of CEES that passed through the membrane entered the FID detector and was combusted/quantified and any amount remaining in the feed chamber was removed before any succeeding injection was made. In **Figure 7**a,b, the FID sensor responses are given, showing CEES vapor transport through a) the Control-IPN a) and b) the Tether-IPN. The redox state of the IPNs are indicated along with the CEES challenge amounts in μL (liquid droplet volume).

The FID traces for the Control IPN shows significant, but not dramatic (order-of magnitude or more), differences in CEES diffusion rates through the oxidized and reduced states

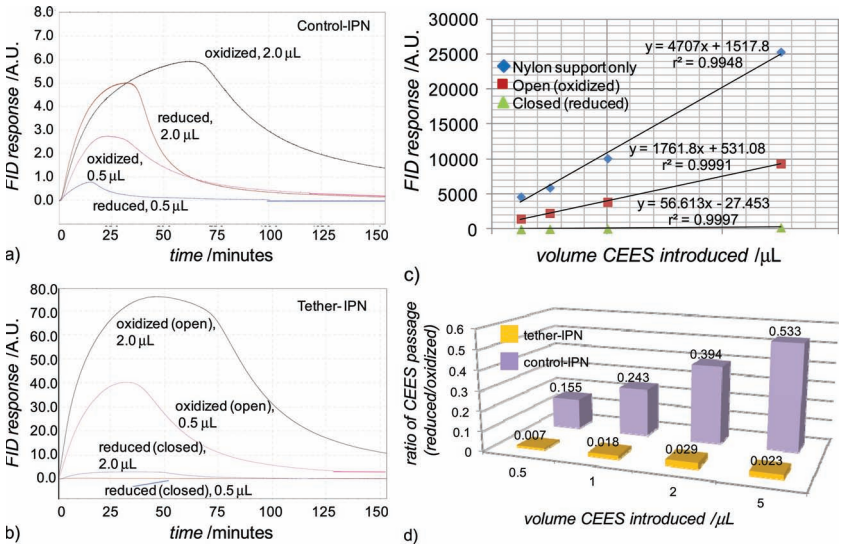

Figure 7. FID sensor responses showing CEES vapor transport through the a) Control-IPN and b) Tether-IPN. The redox state of the IPNs are indicated along with the CEES challenge amounts in µL liquid vaporized. c) Dependence of FID response (in terms of integrated areas under the traces) on CEES challenge amount. Error bars are ±8% to 12%. d) Ratio of CEES passage through the reduced vs. oxidized states of the IPNs. T = 40 °C, relative humidity = 50%. Error bars are ±14%.

of the material. The differences are not surprising since conducting polymers such as polythiophenes are being studied for use as actuators (see Introduction). The change in redox state leads to differences in polymer chain rigidity and packing density, which results in a moderately expanded oxidized form and a more densely packed reduced form. At the challenge level of 0.5 µL CEES, the reduced form of the Control IPN is able to block most of the CEES passage.

The FID traces for the Tether-IPN show an enormous (greater than one order of magnitude) difference in the diffusion rates through the two redox states of the material. The difference is the most pronounced for the lower challenge level of 0.5 µL CEES, where virtually none of the simulant passes through the Tether-IPN closed (reduced) state. Note also the ordinate scale change between Figure 7a,b. The amount of CEES permitted to pass by the closed state Tether-IPN is slightly less that the amount permitted by the Control-IPN reduced state. However, the oxidized (open) Tether-IPN allows much more simulant passage than the oxidized Control-IPN. This is consistent with its much higher MVT rate vs. the oxidized Control-IPN. These comparisons show that the Tether-IPN material is superior to the Control-IPN, both in terms of CEES blockage when reduced and in terms of MVT when oxidized. They also reveal the versatile importance of the tether, which probably plays key roles in the switching of the material, the blocking of CEES transport, and the transport of water vapor through the material.

Figure 7c was constructed for the Tether-IPN, and shows the dependence of FID response (in terms of integrated areas under the traces, up to time = 100 minutes) on CEES challenge amount, in the range 0.5 µL to 5 µL. During data collection, each data point was collected in triplicate, with an experimental error of ± 8% to 12%.The amount of CEES transport allowed by the nylon support by itself is shown in comparison with the amounts allowed by the open and closed IPN states. It is striking that the relationship between CEES challenge amount and vapor detection amount is nearly perfectly linear for both the open and closed states. This indicates that CEES diffusion in the material is likely not cooperative in nature–in other words, individual CEES molecules probably do not interact with each other in ways that increase or decrease their bulk transport rates. The linearity also shows that 1) CEES probably does not react, either with itself or the IPN, as it diffuses through the IPN, and 2) the nature of the barrier to CEES diffusion is best described as mechanical obstruction by the IPN polymers, rather than by specific chemisorptive bonding interactions at chemically distinct sites which would become saturated at higher CEES doses and permit relatively faster diffusion at those dose levels. Finally, repeated exposure to the CEES during testing evidently did not cause the Tether-IPN to change its properties in any way to affect CEES diffusion.

In Figure 7d, the ratios of CEES vapor fluxes through the reduced vs. oxidized states of the open vs. closed IPNs are shown. At the challenge level of 0.5 µL, the ratio is 0.007 (0.7%) for the Tether-IPN. Thus its closed state permits ~140-fold less CEES passage than its open state. As the challenge level is increased to 5 µL, this ratio remains near 2% to 3%. In contrast, the ratio for the Control-IPN steadily increases to ~0.5. This suggests that fundamentally different mechanisms govern CEES diffusion in the Tether-IPN vs. the Control-IPN.

Figure 8a shows CEES vapor passage through the open, closed, and re-opened Tether-IPNs expressed as ratios vs. an expanded Teflon membrane, ePTFE (T = 40 °C and 50% relative humidity). ePTFE is used in breathable sport clothing and has a relatively high MVT. The initial open state is the IPN in its as-synthesized form. The sample was closed as described previously using an applied –1.0 V potential. After the closed sample was exposed to the CEES vapor, it was re-opened using an applied +1.0 V potential. It was clearly possible to re-open the Tether-IPN, and revert it nearly completely back to its initial

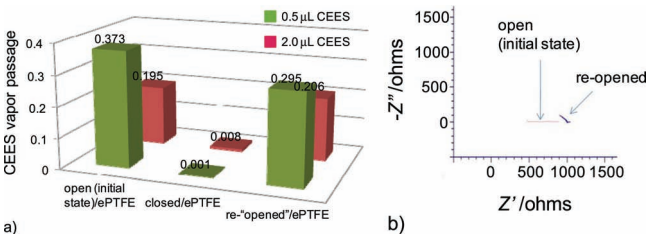

Figure 8. a) CEES vapor passage through the open, closed, and re-opened Tether-IPNs expressed as ratios vs. an expanded Teflon membrane. T = 40 °C, relative humidity = 50%. Error bars are ±14%. b) Nyquist plot of the impedance responses of the open (initial state) and re-opened Tether-IPNs.

open state. This was demonstrated using both levels of the CEES challenge (0.5 and 2 µL). Both the open state materials retard simulant diffusion more effectively than ePTFE. At the 0.5 µL challenge level, the open states passed only ~30% to 37% of the CEES that the ePTFE was able to pass. At the higher challenge level of 2.0 µL, the amount passed was reduced to ~20%. In the closed state, at both challenge levels the Tether-IPN permitted less than 1% of the amount that the ePTFE could pass. Figure 8b is the Nyquist plot of the impedance responses of the open (initial state) and re-opened Tether-IPNs. Both open states give very similar impedances, indicating that the IPN is mostly - but not completely - transformed back into its initial open state following the oxidizing voltage application.

Figure 9 shows the diffusion of a different simulant, methyl salicylate (MeS), through the Tether-IPN. MeS has been used to simulate V-series nerve agents as well as mustard gas. The top, blue trace shows the passage through an ePTFE membrane and the two lower traces show passage through the oxidized, open state (black trace) and the reduced, closed state (violet trace) of the Tether-IPN. If the integrated area of the open IPN state is divided by that of the ePTFE, a ratio of 0.04 is obtained. Thus the open IPN permits far less MeS to permeate than the ePTFE. No integration could be performed for the reduced state because the very small signal is practically in background (noise) levels. Also, far less MeS passes through the open IPN than CEES. This may be related to the vapor pressure of the compounds, with the former much lower than the latter (0.2 mm Hg vs 3.4 mm Hg at 25 °C). The difference in MW (220 vs. 153) also may contribute. Also, CEES passes through much more rapidly than MeS, with a transit time of ~ 100 minutes vs. ~500 minutes. The low vapor pressure of the MeS or attractive forces between the polar OEG tethers and the phenolic hydroxyl group/ester function of the MeS may act to slow the transit of MeS through the Tether-IPN.

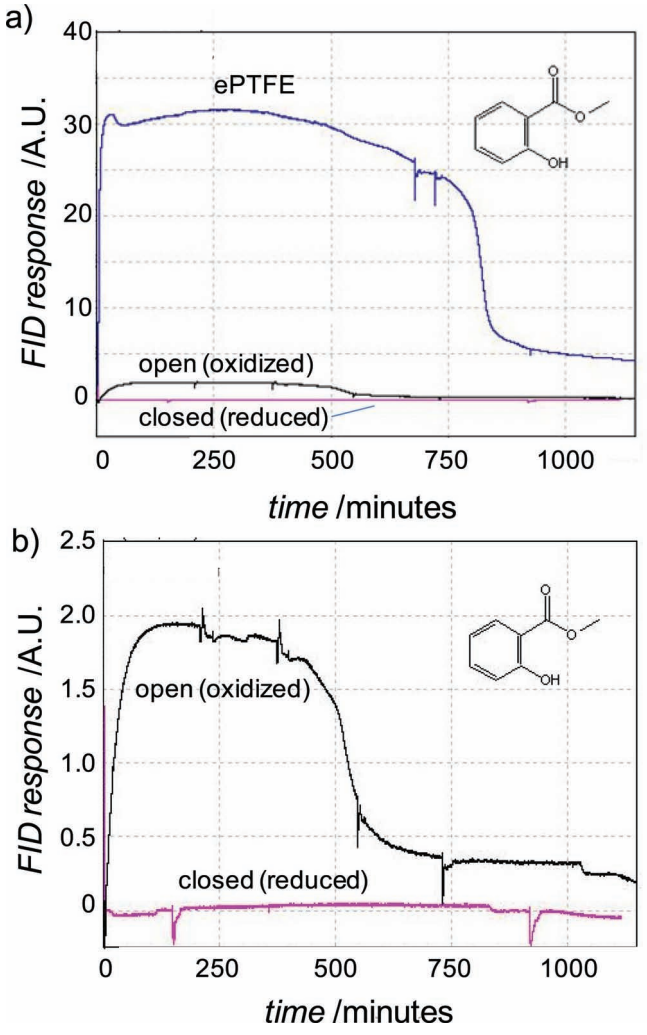

Figure 9. a) FID sensor responses showing MeS vapor transport through ePTFE (top, blue trace) and the Tether-IPN oxidized, open state (black trace) and reduced, closed state (violet trace). The chemical structure of MeS is shown as an inset. T = 40 °C, relative humidity = 50%. b) Enlargement of the lower two traces in (a). The chemical structure of MeS is shown as an inset. T = 40 °C, relative humidity = 50%.

3.8. Composite Durability

We have found that the fabric-supported composite is mechanically strong and quite durable. The nylon support does not appear to experience any degradation during the oxidative polymerization. As mentioned above, we are presently investigating wool as a support fabric and have found that it, too, forms a very durable homogeneous composite with the IPN. It is possible that other relevant fabrics such as Kevlar may also be well-suited as a support.

3.9. Open-Close Mechanism

The Tether-IPN is able to adopt open and closed states that are dramatically different, much more so than those of the Control-IPN. For this effect to occur, the tethers are clearly necessary. We propose a model wherein the CP component of the Tether-IPN experiences a collapse phenomenon when reduced, a behavior very much like that of other poly(thiophenes) and PEDOTs. This collapse process is reversible. In our model, the tethers block the interstitial spaces between the CP and polyurethane chains. In a second part of our model, the RTIL is a key component of the switching process that allows the IPN to be transformed from an open to a closed state, and vice-versa. Here, when the RTIL is absorbed into the IPN, it is dispersed among the tether chains and water molecules that are naturally present in the IPN. These assist in the partial dissociation of the RTIL, allowing it to participate in the redox processes necessary for IPN switching.

It is known that when PEDOT is in its reduced state, the aromatic repeat units experience van der Waals attraction, causing neighboring chains to pack together in dense aggregates.[37] In our model of the Tether-IPN actuation, when the sulfonated tether side chains are oriented by the oxidized CP state in self-doping configurations, neighboring CP main chains are largely masked from one another. Thus they do not aggregate. The IPN is in its open state. Since the tethers are anchored at both ends, their configurational entropy is relatively low. This may impede their ability to block diffusion of small molecules. When the CP

is switched into its reduced state, the CP main chain becomes electrically neutral, and the charged termini of the tethers are released. The CP main chains become exposed to one another, and they begin to pi-stack and aggregate. The freed tethers have a higher configurational entropy and block the interstitial spaces between the CP chains and the polyurethane chains. Their high entropy also may allow them to become more effective in impeding diffusion of small molecules. The CP now resembles a classical polymer "brush". Also, the termini may experience mutual repulsion because of their like negative charges. This would cause them to distribute themselves through the nanoscale spaces in a relatively homogeneous manner, improving the ability of the IPN to block transport of small molecules. This scenario is consistent with what is seen in the TEM images of Figure 3a,b. Finally, the aromatic regions of the CP main chain may aggregate with the aromatic bis-benzamides of the polyurethane chains, enhancing the collapse process of the entire IPN. This phenomenon is depicted in **Figure 10**. The denser nature of the closed vs. open IPN is also quantified by the nitrogen absorption studies summarized in Table 1, and the water absorption studies described above.

For the switching to occur, the RTIL component of the IPN is important. It is present at levels of ~6 wt%, which corresponds to about a 1:1 molar ratio with the OEG-sulfonate tether. Ionic liquids such as Emim-Tf_2 have very low vapor pressures, and thus have extremely low evaporation rates. For our application, it appeared to be an excellent choice for at least two reasons. First, the cationic imidazolium is known to form complexes with the (σ^-) oxygens of polyethylene glycol or OEG,[40–42] which would help localize the RTIL molecules in the regions around the tethers and in close proximity to the CP main chains. Second, the Tf_2 anion can readily exist as a free ion. This allows the Emim cation to provide charge compensation for the freed sulfonate tethers when the IPN is in its closed state. The large size of the Tf_2 anion and the presence of the electron-withdrawing fluorination contribute to delocalization of the electron density, and consequently high polarizability. Electrical conductivity data gathered for ionic liquids with the Tf_2 anion show pronounced ion dissociation, with ionic conductivities similar to electrolyte solutions used in electrochemistry.[43–46] These RTILs have recently been found to dissociate to an additional degree when diluted by addition of 10% v/v water, demonstrating ~14% dissociation at 25 °C.[46] Because of the hydrophilic nature of the sulfonated OEG tether chains, the IPN contains a small fraction of water, determined to be 5 to 7 wt% by thermogravimetric analysis (data not shown). Simulations and spectroscopic studies have shown that Tf_2 interacts strongly with water solute, forming Tf_2…HOH…Tf_2 hydrogen-bonding complexes that stabilize the lone anion.[47] Therefore, the presence of small quantities of water within the IPN fabric

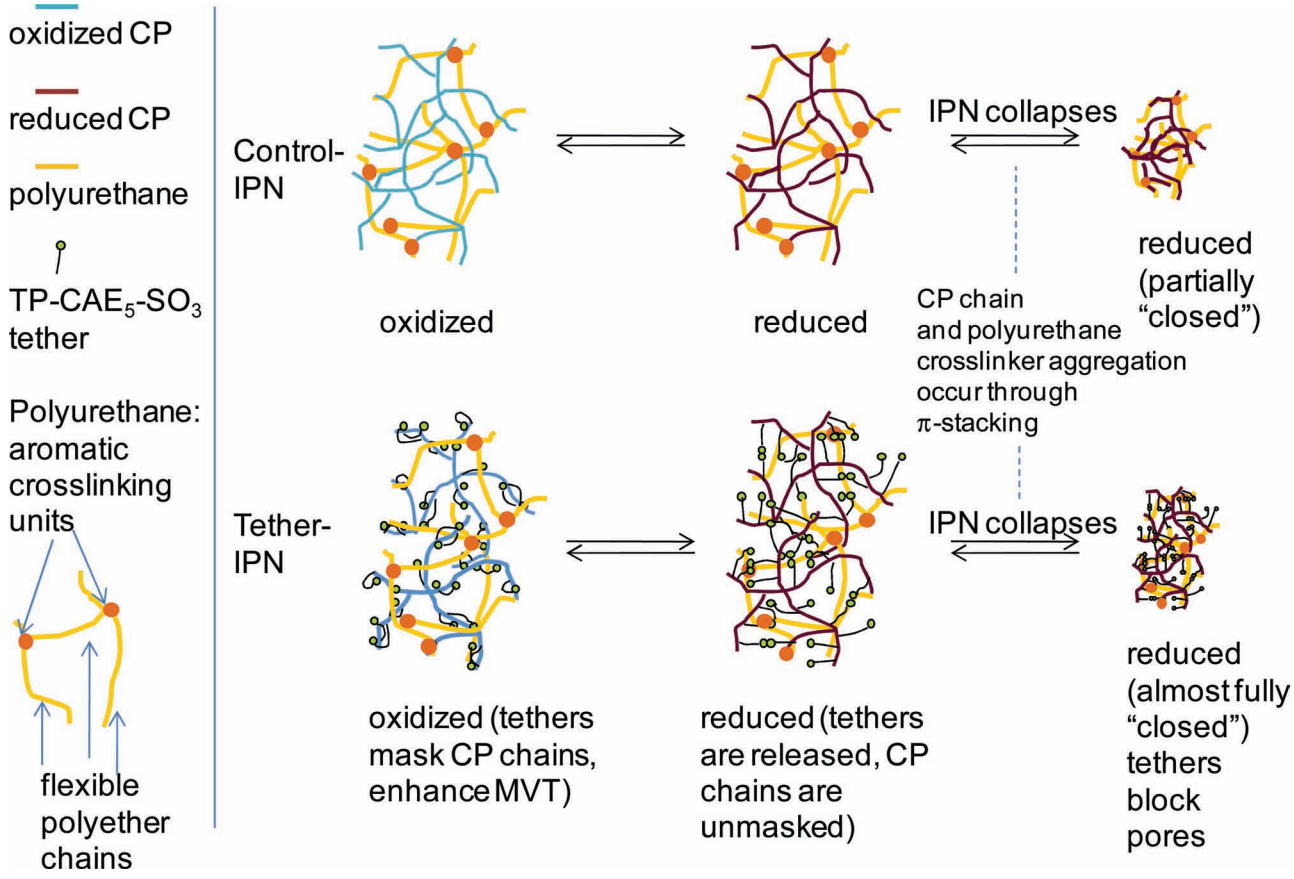

Figure 10. Proposed open-close mechanism showing IPN collapse in both the Control- and Tether-IPNs during redox switching.

would permit this interaction and facilitate anion stabilization. Finally, surface tension studies on Tf_2-containing ILs show that dispersion forces between all species are strong enough to allow the fluid to behave thermodynamically like an ionic solution, allowing the appearance of free ions.[43] We suggest that the ability of the Emim-Tf_2 RTIL to readily dissociate in this manner enables the IPN to be switchable as a macroscopically "dry" material, in the absence of bulk liquid electrolyte.

4. Conclusions

In conclusion, we have developed a switchable IPN material composed of polyurethane and a poly(thiophene-EDOT)-type conducting polymer. The material can be switched between an open, breathable state that rapidly transports water vapor and a closed, protective state that blocks diffusion of chemical agent simulants. Diffusion of CEES simulant was up to 140-fold slower through the closed vs. open states of the IPN. The switching, actuated by application of a small voltage, does not require that conventional liquid electrolyte be present, but is instead facilitated by the presence of a room-temperature ionic liquid with very low volatility. The tether plays an essential role in ensuring a high moisture vapor transport rate (breathability) in the open state material and blocking simulant diffusion, but plays a minimal role in closed state moisture vapor transport. The material could be used in many applications, including breathable, comfortable clothing designed to protect against chemical warfare agents.

5. Experimental Section

5.1. Materials and Instrumentation

MVT75 polyurethane was purchased from Lubrizol Advanced Materials (Wickliffe, OH). This polyurethane (Figure 1d) was originally formulated by BF Goodrich. Support filters were purchased from Fisher Scientific (Pittsburgh, PA). Filter manufacturers were Sterilitech (Kent, WA; polyethersulfone), General Electric Water and Process Technologies (Trevose, PA; Magna Nylon), and Millipore (Billerica, MA; Teflon). Graphite fibers were purchased from Nippon Graphite Fiber Corp. (Tokyo, Japan). Synthesis of TP-CAE_4P-SO_3, and the crosslinker, octanedioic acid bis-(2,3-dihydro-thieno[3,4-b][1,4]dioxin-2-ylmethyl) ester (referred to as EDOT-ODA-EDOT), were performed as described in Supporting Information. Unless specified, all reagents and solvents were purchased from Aldrich Chemical (Milwaukee, WI) and used as supplied. Analytical thin layer chromatography was performed on glass silica plates (E. Merck silica gel 60-F254 with a thickness of 0.25 mm), using the solvent mixture indicated. Preparative chromatographic purifications were performed by employing flash chromatography on E. Merck 40-63 μm normal phase silica gel. Tetraethyleneglycol monoamine was obtained from Molecular BioSciences, Inc. (Colorado). The alcohol precursor, 2,3-dihydrothienol[3,4-b][1,4]dioxin-2-yl methanol (EDOT-CH_2OH), and 3,4 ethylenedioxythiophene (EDOT) were purchased from Sigma-Aldrich (St Louis, MO). ^{1}H NMR spectra were recorded on a Bruker DRX-400 spectrometer in $CDCl_3$ or D_2O solutions. Two-chambered diffusion cells were purchased from Permeagear (Bethlehem, PA). Humidity indicators were purchased from Testo Inc. (Sparta, NJ). Potentiostats (Model 760 D) were purchased from CH Instruments (Austin, TX). The Thermogravimetric Analyzer (Model 2950) was purchased from TA Instruments (New Castle, DE). The GC oven and FID apparatus (Model 2010) was purchased from Shimadzu Scientific Instruments (Columbia, MD). TEM images were obtained using a 200 keV JEOL 2200FS transmission electron microscope. Nitrogen adsorption experiments were performed on a Micromeritics ASAP 2010 porosimeter at 77 K (Micromeritics Instrument Corporation, Norcross, GA). Samples were degassed to 1 mm Hg at 70 °C prior to analysis.

5.2. Chemical Syntheses

Synthesis of IPN Precursors: The synthesis procedures for TP-CAE_4P-SO_3, EDOT-ODA-EDOT, and DMTP are given in ´the Supporting Information.

IPN Synthesis in Filter Supports: The filter-supported IPN was synthesized by blending a polyurethane-containing solvent with a second solvent containing EDOT-ODA-EDOT, EDOT, and carbon fibers. This mixture was then blended with a third solvent containing TP-CAE_4P-SO_3, and iron (III) tosylate oxidant. The final mixture was then cast into a support filter, which was then heated to polymerize the thienyl termonomers in an oxidative, statistical terpolymerization. The procedure is a variation of that reported for IPN synthesis using underivatized EDOT and polyurethane.[48] Adherent IPNs were formed in filters composed of nylon (0.1 μm pore size). The nylon filters were originally circular in shape (4.7 cm diameter), and prior to use were cut into quadrants of equal area (4.3 cm^2 each), weighing ~24 mg. In a typical synthesis, 240 μL of THF containing 10 wt% polyurethane was added to 160 μL anisole containing 6 mg EDOT-ODA-EDOT, 4 μL EDOT, and 10 mg carbon fibers (Granoc, 50 micron avg. length, Nippon Graphite Fiber Corp.) forming solution "1". The mixing was performed in a 1-cm diameter 2.5 ml vial. Next, 140 μL ethanol containing 24 mg TP-CAE_4P-SO_3 was added to 200 μL ethanol containing 120 mg iron (III) tosylate hexahydrate oxidant, forming solution "2", again in a 1-cm diameter 2.5 ml vial. Solutions 1 and 2 were then mixed vigorously (2 was added to 1). To permit full solubility of the polyurethane component, an additional 160 μL THF was added. The mixing was performed for an additional 30 minutes at 35 °C, at 1200 RPM using a small magnetic stir bar. Finally, four 150 to170 μL aliquots of the blended solution were then separately deposited onto 4 cut filter supports (the sections were resting on a glass microscope slide, both the sections and the slide were pre-heated in the oven at 70 °C). The deposition was done by pipette, and the solution was deposited in a manner allowing complete and uniform coverage of the filter, without solution runoff. The polymerization was allowed to proceed overnight at 70–75 °C. The IPN formed in the filter support and was dark blue in color because of the oxidized poly((TP-CAE_4-SO_3)/EDOT-ODA-EDOT/EDOT). The samples were carefully removed from the glass slide and immersed in hot water for 30 seconds (stirring, 80–85 °C) to extract the iron (II) reaction byproduct as well as any unreacted iron (III). Thermogravimetric analysis was performed using a TA Instruments Model 2950 Thermogravimetric Analyzer with a temperature ramp of 10 °C/min in the range 25 °C to 600 °C. The results showed that the extraction procedure removed ~98% of the iron salts from the samples. The samples were then air-dried and stored at room temperature. Each filter section was found to contain ~13.5 mg of the IPN. Finally, the ionic liquid component was introduced by pipetting a 30 wt% solution of 1-ethyl-3-methyl imidazolium-bis-(perfluoroethylsulfonyl) imide ionic liquid in ethanol to the filter section, and the solution was permitted to dry at 25 °C. For the IPN synthesis, the overall wt% yield was 86%–87%.

5.3. Electrochemical Impedance Spectroscopy

Electrochemical switching and EIS measurements were performed using a two-electrode configuration, with the working and counter electrodes attached to opposite ends of the IPN sample, which had a typical size of 1.5 cm × 1.5 cm. The reference and counter electrodes were shorted as is typically done for two-electrode impedance measurements. The working

and counter electrodes were interfaced onto the surface of the sample through thin strips of highly conductive copper metal (sheet resistance ~ 1 Ohm), dimensions 3 mm × 10 mm × 0.1 mm.

5.4. Water Absorption Studies

An 8 μL (+/–0.25 μL) droplet of water was carefully applied to the surface of an IPN in its oxidized and reduced state. Video acquisition was made at a frame rate of 15.2 frames per s (0.066 s per frame) and was begun before the droplet made contact with the surface of the IPN. Video acquisition was completed once the water droplet was completely absorbed by the material. Based on the time stamp for each frame, an absorption rate was calculated for the oxidized and reduced states of the IPN. Video acquisition was performed using a VCA contact angle system 2500 (VCA2500, ASC Products, USA).

Supporting Information

Supporting Information is available from the Wiley Online Library or from the author.

Acknowledgements

G.J. acknowledges the National Research Council for an NRC Postdoctoral Fellowship. The authors wish to thank Evgeniya Locke for helpful technical support. This work was supported by the Defense Threat Reduction Agency, Chemical and Biological Technologies Directorate, program BA07PRO013.

Received: September 20, 2011
Revised: February 10, 2012
Published online: April 24, 2012

[1] Y. Qiu, K. Park, *Adv. Drug Delivery Rev.* **2001**, *53*, 321.
[2] I. Tokarev, S. Minko, *Adv. Mater.* **2009**, *21*, 241.
[3] Q. Fu, G. V. R. Rao, L. K. Ista, Y. Wu, B. P. Andrzejewski, L. A. Sklar, T. L. Ward, G. P. López, *Adv. Mater.* **2003**, *15*, 1262.
[4] B. D. Martin, J. Naciri, M. H. Moore, D. A. Lowy, M. A. Dinderman, E. C. Pehrsson, B. Ratna, *Electrochem. Commun.* **2009**, *11*, 169.
[5] M. A. C. Stuart, W. T. S. Huck, J. Genzer, M. Muller, C. Ober, M. Stamm, G. B. Sukhorukov, I. Szleifer, V. V. Tsukruk, M. Urban, F. Winnik, S. Zauscher, I. Luzinov, S. Minko, *Nat. Mater.* **2010**, *9*, 101.
[6] H. Chen, G. R. Palmese, Y. A. Elabd, *Macromolecules* **2007**, *40*, 781.
[7] R. Liu, Y. Zhang, P. Feng, *J. Am. Chem. Soc.* **2009**, *131*, 15128.
[8] R. Liu, X. Zhao, T. Wu, P. Feng, *J. Am. Chem. Soc.* **2008**, *130*, 14418.
[9] Y. Ito, Y. S. Park, Y. Imanishi, *Langmuir* **2000**, *16*, 5376.
[10] R. Casasús, M. D. Marcos, R. Martínez-Máñez, J. V. Ros-Lis, J. Soto, L. A. Villaescusa, P. Amorós, D. Beltrán, C. Guillem, J. Latorre, *J. Am. Chem. Soc.* **2004**, *126*, 8612.
[11] R. Casasús, E. Climent, M. D. Marcos, R. Martínez-Máñez, F. Sancenón, J. Soto, P. Amorós, J. Cano, E. Ruiz, *J. Amer. Chem. Soc.* **2008**, *130*, 1903.
[12] E. Aznar, M. D. Marcos, R. n. Martínez-Mañez, F. l. Sancenón, J. Soto, P. Amorós, C. Guillem, *J. Am. Chem. Soc.* **2009**, *131*, 6833.
[13] T. K. Tam, M. Ornatska, M. Pita, S. Minko, E. Katz, *J. Phys. Chem. C* **2008**, *112*, 8438.
[14] J. A. Halldorsson, S. J. Little, D. Diamond, G. Spinks, G. Wallace, *Langmuir* **2009**, *25*, 11137.
[15] M. Pyo, J. R. Reynolds, L. F. Warren, H. O. Marcy, *Synth. Met.* **1994**, *68*, 71.
[16] B. L. Fletcher, S. T. Retterer, T. E. McKnight, A. V. Melechko, J. D. Fowlkes, M. L. Simpson, M. J. Doktycz, *ACS Nano* **2008**, *2*, 247.
[17] G. Jeon, S. Y. Yang, J. Byun, J. K. Kim, *Nano Lett.* **2011**, *11*, 1284.
[18] M. R. Abidian, D. H. Kim, D. C. Martin, *Adv. Mater.* **2006**, *18*, 405.
[19] E. Smela, N. Gadegaard, *Adv. Mater.* **1999**, *11*, 953.
[20] J. Ficker, A. Ullmann, W. Fix, H. Rost, W. Clemens, *J. Appl. Phys.* **2003**, *94*, 2638.
[21] V. Seshadri, L. Wu, G. A. Sotzing, *Langmuir* **2003**, *19*, 9479.
[22] C.-C. Chang, L.-J. Her, J.-L. Hong, *Electrochim. Acta* **2005**, *50*, 4461.
[23] I. Luzinov, S. Minko, V. V. Tsukruk, *Soft Matter* **2008**, *4*, 714.
[24] J.-F. Lutz, *Adv. Mater.* **2011**, *23*, 2237.
[25] J. Ouyang, Q. Xu, C.-W. Chu, Y. Yang, G. Li, J. Shinar, *Polymer* **2004**, *45*, 8443.
[26] B. D. Martin, N. Nikolov, S. K. Pollack, A. Saprigin, R. Shashidhar, F. Zhang, P. A. Heiney, *Synth. Met.* **2004**, *142*, 187.
[27] K. Ito, Y. Tominaga, H. Ohno, *Electrochim. Acta* **1997**, *42*, 1561.
[28] *Handbook of Conducting Polymers*, (Ed: T. A. Skotheim) Marcel Dekker, New York **1998**.
[29] A. O. Patil, Y. Ikenoue, F. Wudl, A. J. Heeger, *J. Am. Chem. Soc.* **1987**, *109*, 1858.
[30] G. R. Lomax, *J. Mater. Chem.* **2007**, *17*, 2775.
[31] M. Dobbelin, R. Marcilla, C. Pozo-Gonzalo, D. Mecerreyes, *J. Mater. Chem.* **2010**, *20*, 7613.
[32] M. Döbbelin, R. Tena-Zaera, R. Marcilla, J. Iturri, S. Moya, J. A. Pomposo, D. Mecerreyes, *Adv. Funct. Mater.* **2009**, *19*, 3326.
[33] D. M. Tigelaar, J. R. Waldecker, K. M. Peplowski, J. D. Kinder, *Polymer* **2006**, *47*, 4269.
[34] H. H. Kuhn, A. D. Child, W. C. Kimbrell, *Synth. Met.* **1995**, *71*, 2139.
[35] D. Mecerreyes, V. Alvaro, I. Cantero, M. Bengoetxea, P. A. Calvo, H. Grande, J. Rodriguez, J. A. Pomposo, *Adv. Mater.* **2002**, *14*, 749.
[36] W. Torres, J. C. Donini, A. A. Vlcek, A. B. P. Lever, *Langmuir* **1995**, *11*, 2920.
[37] T. F. Otero, M. Caballero Romero, *Polym. Int.* **2010**, *59*, 329.
[38] P. Gibson, H. Schreuder-Gibson, "Influence of hydration state on permeation testing and vapor transport properties of polymer films", presented at *International Nonwovens Technical Conference*, Denver, CO, 21-24th September, 2009.
[39] P. W. Gibson, *Polym. Test.* **2000**, *19*, 673.
[40] S. K. Chaurasia, R. K. Singh, S. Chandra, *Solid State Ionics* **2011**, *183*, 32.
[41] F. Maier, T. Cremer, C. Kolbeck, K. R. J. Lovelock, N. Paape, P. S. Schulz, P. Wasserscheid, H. P. Steinruck, *Phys. Chem. Chem. Phys.* **2010**, *12*, 1905.
[42] T.-Y. Wu, B.-K. Chen, L. Hao, Y.-C. Peng, I.-W. Sun, *Int. Jr. Molec. Sci.* **2011**, *12*, 2598.
[43] F. Leroy, V. C. Weiss, *J. Chem. Phys.* **2011**, *134*, 094703.
[44] M. G. Freire, P. J. Carvalho, A. M. Fernandes, I. M. Marrucho, A. J. Queimada, J. A. P. Coutinho, *J. Colloid Interface Sci.* **2007**, *314*, 621.
[45] A. M. Fernandes, M. A. A. Rocha, M. G. Freire, I. M. Marrucho, J. o. A. P. Coutinho, L. s. M. N. B. F. Santos, *J. Phys. Chem. B* **2011**, *115*, 4033.
[46] P. Wang, A. Anderko, *Fluid Phase Equilib.* **2011**, *302*, 74.
[47] H. Weingärtner, *Angew. Chem. Int. Ed.* **2008**, *47*, 654.
[48] T. S. Hansen, K. West, O. Hassager, N. B. Larsen, *Adv. Funct. Mater.* **2007**, *17*, 3069.